Molecular mechanism underlying the TLR4 antagonistic and antiseptic activities of papiliocin, an insect innate immune response molecule

Manigandan Krishnan[a,1], Joonhyeok Choi[a,1], Ahjin Jang[a], Sungjae Choi[a], Jiwon Yeon[a], Mihee Jang[a], Yeongjoon Lee[a], Kkabi Son[a], Soon Young Shin[b], Myeong Seon Jeong[c], and Yangmee Kim[a,2]

[a]Department of Bioscience and Biotechnology, Konkuk University, Seoul 05029, South Korea; [b]Department of Biological Sciences, Konkuk University, Seoul 05029, South Korea; and [c]Chuncheon Center, Korea Basic Science Institute, Chuncheon 24341, South Korea

Edited by Michael Strand, Department of Entomology, University of Georgia, Athens, GA; received September 7, 2021; accepted January 13, 2022

Antimicrobial peptides are innate immune molecules playing essential roles in insects, which lack the adaptive immune system. Insects possess Toll9, the innate pattern-recognition receptor highly similar to the mammalian Toll-like receptor 4 (TLR4), which is involved in recognizing lipopolysaccharide (LPS). TLR4 is an important therapeutic target, as it causes uncontrolled immune response in sepsis; therefore, identification of TLR4-targeting molecules is imperative. Papiliocin, an insect cecropin derived from the larvae of the swallowtail butterfly, possesses potent antibacterial activities against gram-negative bacteria. We investigated the molecular mechanism underlying the TLR4-antagonistic and antiseptic activities of papiliocin. Binding analysis, docking simulation, and flow cytometry showed that papiliocin inhibited LPS-induced TLR4 signaling by directly binding to TLR4/MD-2 and causing rapid dissociation of LPS from the TLR4/MD-2 complex. R13 and R16 in the N-terminal helix, conserved in insect cecropins, were the key binding sites at the TLR4/MD-2 interface, along with the flexible hinge region, which promoted the interaction of the hydrophobic carboxyl-terminal helix with the MD-2 pocket to competitively inhibit the LPS–TLR4/MD-2 interaction. Papiliocin, an antiendotoxin molecule and TLR4 inhibitor, rescued the pathology of *Escherichia coli*–induced sepsis in mice more effectively and with lower nephrotoxicity compared to polymyxin B. Our results provide insight into the key structural components and mechanism underlying the TLR4-antagonistic activities of papiliocin, which is essential for the innate immune response of the insect against microbial infection. Papiliocin may be useful for developing a multifunctional alternative to polymyxin B for treating gram-negative sepsis.

insect cecropin | Toll-like receptor 4 | LPS | antimicrobial peptide | insect innate immunity

Toll-like receptors (TLRs) are innate immune receptors that recognize pathogen-associated molecular patterns to protect the host from invading pathogens (1). TLR4 is one of the most critical pattern-recognition receptors in the TLR family that recognizes lipopolysaccharide (LPS) released from the outer membrane of gram-negative bacteria to elicit innate immune response (2). Subsequently, an LPS-binding protein attracts LPS and facilitates CD14-dependent transfer of LPS to TLR4 via the adaptor protein MD-2, resulting in dimerization of the TLR4/MD-2 complex. The dimer mediates translocation of nuclear factor-kappa B (NF-κB), ultimately resulting in the production of proinflammatory cytokines. Therefore, uncontrolled LPS-induced inflammatory TLR4 signaling can cause acute sepsis (3). Sepsis induced by multidrug-resistant gram-negative bacteria, such as carbapenem-resistant bacteria, is difficult to eradicate and causes serious health issues (4, 5), as carbapenems such as imipenem, doripenem, and meropenem are generally the final choices for treating infections caused by gram-negative bacteria. As management of carbapenem-resistant *Pseudomonas aeruginosa*, *Acinetobacter baumannii*, and *Enterobacteriaceae* including *Klebsiella pneumoniae* and *Escherichia coli* is extremely difficult, the World Health Organization has prioritized the development of methods for effectively treating infections caused by these pathogens (6, 7). Research in this field has mainly focused on developing antiseptic molecules that can either clear bacterial LPS or competitively target the binding of LPS to TLR4/MD-2, resulting in inhibition of the TLR4 signaling pathway (8–10). Therefore, molecules with dual effects can be advantageous for inhibiting systemic TLR4-mediated inflammatory sepsis.

Antimicrobial peptides (AMPs) are important natural components of the innate immune system in various organisms (11) and typically kill pathogens by permeabilizing their membranes or targeting intracellular components (12). In addition, AMPs can modulate the host immune system via multiple pathways (13). Therefore, AMPs have emerged as effective molecules against multidrug-resistant bacteria and potential alternatives to conventional antibiotics for treating gram-negative infections (14). Polymyxin B (PMB) and colistin are cyclic cationic AMPs, which are used as a last resort for treating gram-negative infections (15). PMB prevents gram-negative sepsis by removing bacterial LPS. However, increased resistance, nephrotoxicity, and neurotoxicity associated with PMB have limited its use in clinical practice (16).

Significance

Similar to mammalian TLR4/MD-2, the Toll9/MD-2–like protein complex in the silkworm, *Bombyx mori,* acts as an innate pattern-recognition receptor that recognizes lipopolysaccharide (LPS) and induces LPS-stimulated expression of antimicrobial peptides such as cecropins. Here, we report that papiliocin, a cecropin-like insect antimicrobial peptide from the swallowtail butterfly, competitively inhibits the LPS-TLR4/MD-2 interaction by directly binding to human TLR4/MD-2. Structural elements in papiliocin, which are important in inhibiting TLR4 signaling via direct binding, are highly conserved among insect cecropins, indicating that its TLR4-antagonistic activity may be related to insect Toll9-mediated immune response against microbial infection. This study highlights the potential of papiliocin as a potent TLR4 antagonist and safe peptide antibiotic for treating gram-negative sepsis.

Author contributions: Y.K. designed research; M.K., J.C., A.J., S.C., J.Y., M.J., Y.L., K.S., S.Y.S., and M.S.J. performed research; M.K., J.C., A.J., S.C., J.Y., M.J., Y.L., K.S., and Y.K. analyzed data; and M.K., J.C., and Y.K. wrote the paper.

The authors declare no competing interest.

This article is a PNAS Direct Submission.

[1]M.K. and J.C. contributed equally to the work.

[2]To whom correspondence may be addressed. Email: ymkim@konkuk.ac.kr.

This article contains supporting information online at http://www.pnas.org/lookup/suppl/doi:10.1073/pnas.2115669119/-/DCSupplemental.

Published March 1, 2022.

Insects are extremely resistant to microbial infections owing to their strong innate immune system, which includes the production of AMPs (17). In insects, Toll was initially identified in *Drosophila melanogaster* as an integral membrane receptor (18). Insect Toll is highly similar to mammalian TLR, and Toll/TLRs are considered key regulators of the innate immune system in both insects and mammals (19). A recent study showed that in the silkworm, *Bombyx mori*, Toll9 recognizes LPS by interacting with two MD-2–related lipid recognition domains, named Toll9/MD-2A or Toll9/MD-2B, indicating their functional and evolutionary similarity with mammalian TLR4/MD-2 proteins (20, 21). Insect Toll9 may be a pattern-recognition immune receptor similar to mammalian TLR4 in complex with MD-2 during LPS recognition and signaling (21). Cecropins are a group of widely studied AMPs that play important roles in the innate immune response of insects (22–24). In 1981, Steiner et al. reported that cecropins are produced from the hemolymph of bacterially challenged diapausing pupae of the giant silk moth, *Hyalophora cecropia* (25). Since then, several cecropin-like peptides have been identified in insects such as *B. mori* (26) and *D. melanogaster* (24). In *B. mori,* LPS can activate the expression of AMPs such as cecropin B, moricin, lebocin3, and attacin1 (21, 27). Some insect cecropins have shown potent antibacterial activities and in vivo antiseptic activities, confirming their therapeutic potential (23, 28–31).

Papiliocin, an AMP belonging to the insect cecropin family, was isolated from the larvae of the swallowtail butterfly, *Papilio xuthus* (32). We previously showed that papiliocin has broad-spectrum antibacterial activity—particularly against gram-negative bacteria—in which it disrupts the bacterial membrane, similar to other insect cecropins (33–37). We determined the solution structure of papiliocin, which contains two α-helices: an amphipathic N-terminal helix from R1 to K21 and a hydrophobic carboxyl-terminal helix from A25 to V37, separated by a hinge region (33). Most insect cecropins share this helix–hinge–helix structure with high sequence homology. Furthermore, papiliocin inhibits nitric oxide (NO) production and may suppress tumor necrosis factor (TNF)-α via innate defense response mechanisms, which involve the TLR4 pathway in LPS-stimulated RAW 264.7 cells (33). We also found that aromatic residues (W2 and F5), as well as the amphipathic N-terminal helix, play important roles in the membrane permeabilization and anti-inflammatory activities of papiliocin (34, 35). Therefore, using the sequence of the N-terminal helix of papiliocin, short peptide antibiotics, such as the papiliocin–magainin hybrid peptide and a 12-mer peptide, which exhibited a diverse range of antimicrobial activities against gram-negative infections, were designed (36, 37). However, the detailed mechanism underlying TLR4 signaling inhibition and the role of the conserved hydrophobic carboxyl-terminal helix remain unclear.

Considering the emerging role of TLR4 in the progression of gram-negative bacterial infections to sepsis and the urgent need to find safe antiseptic alternatives to PMB for clinical use, we investigated the molecular mechanism of action of papiliocin as a TLR4 inhibitor using binding analysis, docking simulation, saturation transfer difference (STD) NMR, and flow cytometry. This study demonstrates the role of the conserved structural components of insect cecropins involved in direct binding to TLR4/MD-2, preventing its dimerization and thereby inhibiting the LPS-stimulated TLR4 inflammatory signaling pathway. This study also provides insight into the mechanism underlying the human TLR4-antagonistic activities of papiliocin, which may be essential for understanding the functionally similar Toll9/MD-2–mediated insect innate immune response against microbial infection. The antiseptic effect and low nephrotoxicity of papiliocin were confirmed using in vivo sepsis models and compared to that of PMB, highlighting its potential as a safe alternative to PMB for treating gram-negative sepsis.

Results

Papiliocin Is a Potent LPS-Neutralizing Peptide. Considering the high selectivity of papiliocin for gram-negative bacteria and its anti-inflammatory effect (33), we examined whether these properties are related to its LPS-neutralizing properties similar to that of PMB, which is a well-known LPS-neutralizing peptide that prevents endotoxin shock. Therefore, we investigated its LPS-binding and -neutralizing properties and compared them to those of PMB. Using a BODIPY-cadaverine (BC) displacement assay, we found that 2 μM papiliocin displaced 74.6% of the BC probe from LPS, indicating that it was more efficient than PMB (18.8%) and possessed relatively stronger LPS-binding capacity (Fig. 1*A*). Furthermore, limulus amebocyte lysate (LAL) analysis demonstrated that papiliocin remarkably neutralized LPS, which was comparable to the neutralizing activity of PMB (Fig. 1*B*). Isothermal titration calorimetry (ITC) indicated an exothermic process with strong electrostatic interactions; the binding affinity of papiliocin to LPS was 6.3×10^{-8} M, which was higher than that between PMB and LPS (3.3×10^{-7} M) (Fig. 1*C*). Flow cytometry analysis revealed that papiliocin inhibits 52% of fluorescein isothiocyanate (FITC)-LPS binding to the RAW 264.7 cell surface but also competitively displaced prebound LPS in the LPS–receptor complex by 25% on RAW 264.7 cells, whereas PMB had no competitive impact (Fig. 1*D*). These data suggest that papiliocin has a dual mode of interactions with LPS, including a direct binding relationship with LPS as well as elimination LPS after connecting with their receptors.

Papiliocin Specifically Targeted the TLR4-Signaling Pathway in Macrophages. To understand the molecular mechanism via which papiliocin controls the pathogen-induced immune response, we evaluated the specificity of papiliocin for various TLR proteins using TLR-specific agonists that mimic the microbial activation of macrophages. As shown in Fig. 1*E*, papiliocin effectively and selectively reduced LPS-stimulated NO levels by 66.4% and thereby reduced TLR4 signaling, even at 1 μM, but did not affect other TLR-signaling pathways. To further confirm the TLR4-modulating effects of papiliocin, we analyzed the secreted alkaline phosphatase (SEAP) regulatory effect using human embryonic kidney (HEK)-Blue hTLR4 cells. As expected, papiliocin treatment significantly reduced TLR4-mediated SEAP activity, with a low half-maximal inhibitory concentration (IC_{50}) of 1.1 μM (Fig. 1*F*), indicating that it specifically targeted TLR4 signaling. Considering our previous findings regarding the role of papiliocin in TLR4 regulation, we analyzed the levels of TLR4-downstream proteins in LPS-stimulated RAW 264.7 cells using immunoblotting (Fig. 1 *G* and *H*). Papiliocin treatment considerably decreased the overexpression of MyD88 and the phosphorylation levels of TAK1, p38, c-Jun N-terminal kinase (JNK), and extracellular signal-regulated kinase (ERK) in LPS-challenged RAW 264.7 cells. These results suggested that even 0.1 μM papiliocin effectively inhibited the proteins acting downstream of TLR4. Immunocytochemistry showed that papiliocin inhibited LPS-stimulated p-NF-κB p65 translocation (Fig. 1*I*), which was in agreement with the results of Western blotting (Fig. 1 *G* and *H*). Thus, papiliocin blocked the LPS-induced inflammatory cascade by targeting TLR4 and the MAPK pathway and by blocking the nuclear translocation of p-NF-κB.

Papiliocin Directly Binds to the TLR4/MD-2 Complex with Micromolar Affinity. We further confirmed the binding of papiliocin to TLR4 using various biophysical assays. STD NMR revealed the intermolecular interactions between peptide and TLR4/MD-2, resulting in inhibition of LPS binding to TLR4/MD-2 (38). Papiliocin showed significant STD effects on TLR4/MD-2, TLR4, and MD-2 (100:1 molar ratio), confirming their direct interactions (Fig. 2 *A* and *B* and *SI Appendix*, Fig. S1 *A–D*). Particularly,

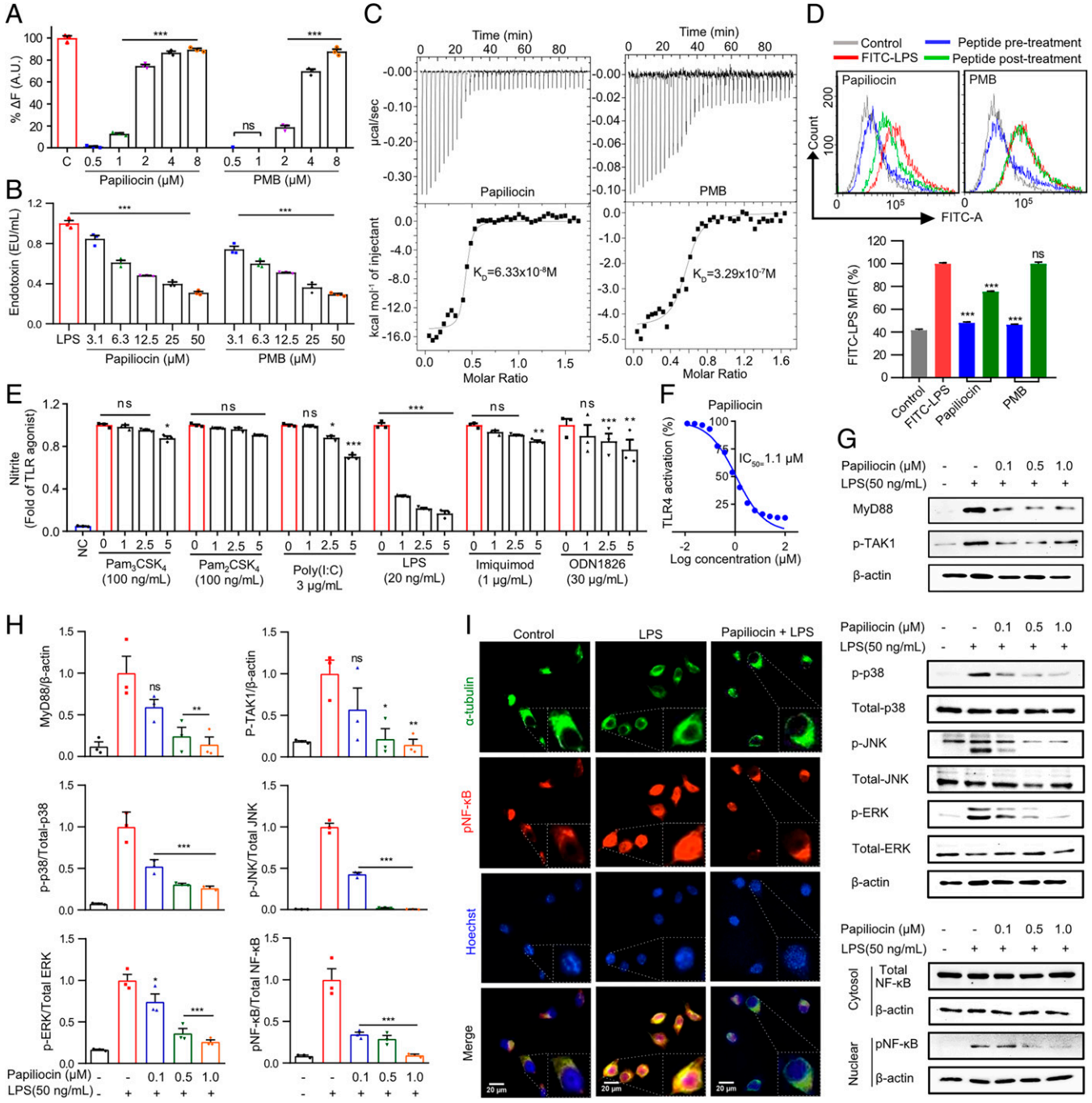

Fig. 1. Papiliocin interacts with LPS and specifically targets TLR4. (*A*) Concentration-dependent (0.5 to 8 μM) BC displacement from LPS after treatment with papiliocin and PMB (LPS, 2 ng/mL; peptides, 3.1, 6.3, 12.5, 25, and 50 μM). (*B*) LAL assay showing the LPS neutralization capacities of papiliocin and PMB. (*C*) ITC measurement showing the binding affinities of papiliocin and PMB to LPS. (*D*) Flow cytometry analysis showing the effect of papiliocin on binding of FITC-LPS to RAW 264.7 cells. Bar graph indicating the mean fluorescence intensity (MFI) of FTIC-LPS surface binding (%) to RAW 264.7 cells. Cells were pretreated (blue) and posttreated (green) with 40 μM peptides (papiliocin and PMB) or 40 μg/mL LPS (red) for 30 min, and the MFI was analyzed using flow cytometry. (*E*) Specificity of papiliocin against various TLRs with TLR-specific agonists determined by monitoring the inhibition of NO production in RAW 264.7 cells. TLR agonist: 100 ng/mL Pam_3CSK_4 (TLR2/1); 100 ng/mL Pam_2CSK_4 (TLR2); 3 μg/mL Poly(I:C) (TLR3); 20 ng/mL LPS (TLR4); 1 μg/mL imiquimod (TLR7), and 30 μg/mL ODN1826 (TLR9) were used to activate selective TLRs; papiliocin (0, 1, 2.5, and 5 μM); NC, negative control. (*F*) Effects of papiliocin (0 to 100 μM) on TLR4 inactivation measured by SEAP assays in LPS (20 ng/mL)-stimulated HEK-Blue hTLR4 cells. (*G*) Effect of papiliocin on suppression of LPS-induced TLR4 and MAPK signaling pathways. RAW 264.7 cells were treated with varying concentrations of papiliocin (0.1, 0.5, and 1.0 μM, 1 h) followed by LPS (50 ng/mL, 30 min) stimulation, and the protein levels were demonstrated by Western blotting. (*H*) Bar graph represents the fold change of corresponding protein levels as analyzed by densitometry. (*I*) Fluorescent images representing the inhibitory effect of papiliocin on the LPS-induced nuclear translocation of p-NF-κB in RAW 264.7 cells. Papiliocin (10 μM, 1 h); LPS (50 ng/mL, 30 min). α-Tubulin is shown in green (Alexa 488), p-NF-κB is shown in red (Alexa 546), and nuclear DNA is blue (Hoechst 33258). Each bar represents mean ± SEM of three independent experiments. $*P < 0.05$, $**P < 0.01$, $***P < 0.001$, and ns, nonsignificant compared with control by one-way ANOVA with Dunnett's comparison test (*A, B, D, E, and H*) and IC_{50} by nonlinear regression analysis (*F*).

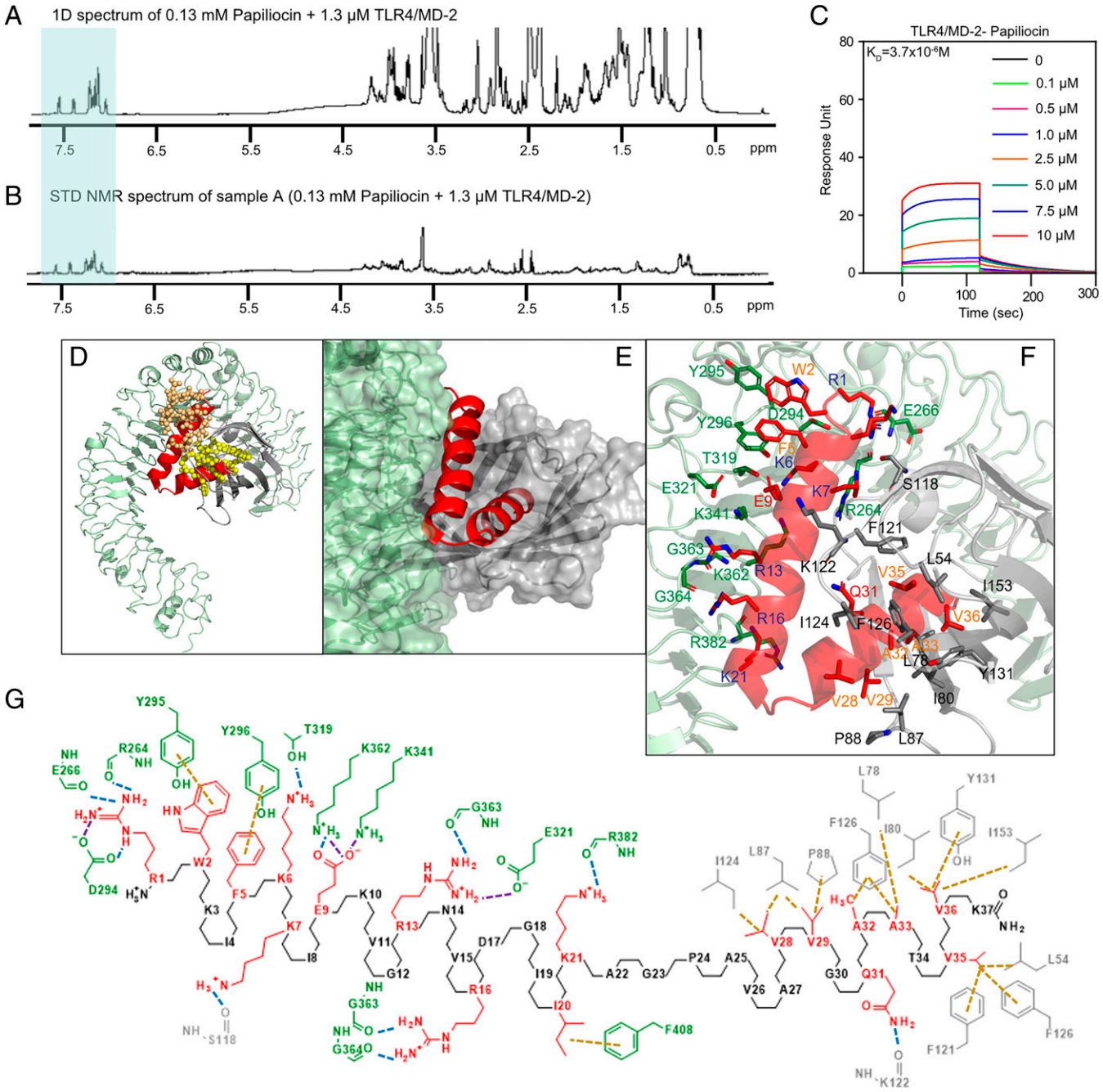

Fig. 2. Binding interaction between papiliocin and TLR4/MD-2. (*A*) One-dimensional ^{1}H NMR spectra of 0.13 mM papiliocin plus 1.3 μM TLR4/MD-2. (*B*) STD NMR spectra were obtained with selective saturation of protein resonances at −3.0 ppm on papiliocin and TLR4/MD-2 (sample A). Aromatic protons of W2 and F5 are marked in the green box. (*C*) SPR sensorgrams of papiliocin binding to TLR4/MD-2. (*D*) Binding model of papiliocin to TLR4/MD-2 complex in ribbon diagram. The crystal structure of the TLR4/MD-2/LPS dimer was overlaied to the papiliocin from the docking model. Papiliocin is in red, TLR4 in green, and MD-2 in gray. Atoms in the head and tail groups of LPS are colored orange and yellow, respectively. (*E*) Close-up surface representation showing the N-terminal helix of papiliocin at the interface of TLR4 and MD-2 and the carboxyl-terminal helix inserted into the hydrophobic cavity of MD-2. (*F*) Important interactions between papiliocin and TLR4/MD-2. (*G*) Two-dimensional illustration of TLR4/MD-2/papiliocin docking, showing hydrogen bonds (blue lines), electrostatic interactions (purple lines), and hydrophobic interactions (brown lines). Residues for papiliocin are denoted in red, and those for TLR4 and MD-2 are in blue and gray, respectively.

well-resolved aromatic protons in W2 and F5 showed strong saturation transfers from TLR4/MD-2 and TLR4, whereas W2 and F5 showed almost no transfer of saturation from MD-2, indicating the critical roles of these aromatic residues at the N-terminal helix in binding interactions with TLR4.

We next measured the binding affinities of papiliocin toward TLR4, MD-2, and the TLR4/MD-2 complex using surface plasmon resonance (SPR). As shown in Fig. 2*C*, papiliocin bound to the TLR4/MD-2 complex with micromolar affinity (3.7×10^{-6} M; association rate = 3,846 $M^{-1} \cdot s^{-1}$, dissociation rate = 0.01409 s^{-1}) and also to both TLR4 and MD-2 with micromolar affinity (4.1×10^{-7} and 1.1×10^{-6} M, respectively; *SI Appendix*, Fig. S2 *A* and *B*). LPS has been shown to bind to TLR4 with 1.41×10^{-5} M binding affinity and to MD-2 with

0.87×10^{-5} M binding affinity (39). Therefore, papilocin may have similar or tighter binding affinity to TLR4 and MD-2 compared to that of LPS. Our results suggested that papiliocin binds directly to TLR/MD-2, contributing to its TLR4 specificity.

Structural Requirement of Papiliocin for Its Antimicrobial Activities. Insect cecropins are composed of helix–hinge–helix structures of 34 to 55 amino acids, the sequences of which are highly homologous (*SI Appendix*, Fig. S3 *A* and *B*). The sequence of papiliocin showed >90% similarity to those of insect cecropins from the moth and butterfly, including the sequence of the highly conserved structural element consisting of two helices separated by a conserved hinge sequence (*SI Appendix*, Fig. S3*A*). The N-terminal α-helix of papiliocin exhibits amphipathic characteristics, with highly conserved lysine, arginine, tryptophan, and phenylalanine residues, whereas the hydrophobic carboxyl-terminal helix contains conserved hydrophobic residues such as alanine and valine. However, the precise functions of the conserved hydrophobic carboxyl-terminal helix are unknown. Therefore, we identified the structural components of papiliocin that contribute to the antibacterial and LPS-binding activities of papiliocin. We next investigated the structural features of papiliocin required for its binding to TLR4/MD2.

Our previous molecular dynamics simulation showed that the flexible Gly-Pro hinge region facilitates the N-terminal helix lying on the surface of the negatively charged bacterial membrane, whereas the carboxyl-terminal helix may be buried in the bacterial membrane (40). To evaluate the role of the flexible hinge region in antimicrobial activities, we designed two hinge analogs (*SI Appendix*, Table S1). In the hinge sequence "G23P24," P24 was replaced with Gly (P24G) to provide higher flexibility, whereas G23 was replaced with Pro (G23P) to increase the rigidity of the hinge region. We evaluated the antibacterial and LPS-binding activities of the N-terminal helix (PapN; R1-A22) and carboxyl-terminal helix (PapC; A25-K37) peptides as well as two analogs with modifications of the hinge sequence (G23P and P24G) (*SI Appendix*, Table S1). Papiliocin (1 μM) killed all *E. coli*, whereas the effect of PapN was considerably weaker (minimum inhibitory concentration [MIC], 16 μM) and PapC showed negligible bactericidal activity even at 64 μM. Notably, the P24G analog exhibited comparable antibacterial properties; however, G23P showed significantly lower (two- to eightfold) antibacterial activity compared to that of papiliocin. Furthermore, analysis of membrane depolarization of intact *E. coli* showed that papiliocin, P24G, PapN, and G23P showed 72.0%, 69.1%, 32.8%, and 26.2% depolarization at 8 μM. PapC did not permeabilize the intact *E. coli* and spheroplast (Fig. 3 *A* and *B*). LAL analysis showed that at 12.5 μM, papiliocin neutralized 52.0% LPS, P24G neutralized 40.6% LPS, and PapN neutralized only 26.8% LPS. Interestingly, PapC and G23P did not neutralize LPS (Fig. 3*C*). The binding affinity measured using ITC confirmed that PapN, which lacks the carboxyl-terminal helix, had 10-fold lower affinity for LPS compared to papiliocin, although PapC did not bind to LPS at all (Fig. 3*D*). Interestingly, P24G with a more flexible Gly-Gly hinge compared to papiliocin showed comparable MIC and 10-fold lower affinity for LPS compared to papiliocin, whereas G23P with a more rigid Pro-Pro hinge showed much lower MIC compared to papiliocin and did not show LPS-binding activities (*SI Appendix*, Table S1 and Fig. 3*D*). Interestingly, papiliocin and P24G depolarized intact *E.coli* membrane much more efficiently compared to spheroplast inner membrane, while G23P depolarized intact *E.coli* membrane much less than papiliocin, which agrees well with their LPS-binding properties and antibacterial activities against *E.coli* (Fig. 3 *A–D*). Therefore, the N-terminal and carboxyl-terminal helices, as well as their connected hinge region with proper flexibility in papiliocin, may be required for the cooperative interaction with LPS, resulting in potent antibacterial activity against gram-negative bacteria.

As PapN retained part of the antimicrobial activities of papiliocin, whereas PapC showed no antibacterial or LPS-binding activities, we predicted that this highly conserved hydrophobic carboxyl terminus is involved in the interaction with TLR4/MD-2. To identify the most favorable region of papiliocin for the interaction with TLR4/MD-2, we measured the binding affinities of the two helical domains with TLR4, MD-2 monomer, and the TLR4/MD-2 complex using SPR. PapN showed binding affinities in the micromolar range toward TLR4/MD-2, TLR4, and MD-2 (*SI Appendix*, Fig. S4 *A–C*), indicating its potential to bind to the interface between TLR4 and MD-2. Interestingly, PapC itself could not bind to any receptor (*SI Appendix*, Fig. S4 *D–F*). We also measured the binding affinities of two hinge analogs, G23P and P24G, with TLR4/MD-2. P24G binds to TLR4/MD-2 with 10-fold lower affinity, whereas G23P binds with 100-fold lower affinity compared to papiliocin, indicating that proper flexibility of the hinge region is also important for the papiliocin–TLR4/MD-2 interaction. (*SI Appendix*, Fig. S5 *A–C*).

To confirm the importance of the N-terminal and carboxyl-terminal helices, as well as the flexible hinge region on TLR4-inhibiting activities, we further examined the SEAP activities of PapN and PapC, alone and in combination, along with G23P and P24G analogs (Fig. 3*E*). Papiliocin exhibited 73.9% SEAP inhibitory activity at 3.1 μM, with IC_{50} of 1.1 μM, which was much stronger than that of PapN (0.3%) and P24G (7.3%). However, G23P and PapC did not inhibit SEAP activity. The effect of cotreatment with PapN and PapC on SEAP activity was similar to that observed with PapN treatment alone. Interestingly, PapC alone could not bind to the receptors, which agrees with the results of the STD NMR and SEAP measurements. Furthermore, papiliocin and P24G showed similar anti-inflammatory activities, whereas PapC and G23P completely lost activities (*SI Appendix*, Fig. S6 *A–C*). These results suggest that the carboxyl-terminal hydrophobic helix and flexible hinge region connecting the two helices are critical for TLR4-inhibiting activity along with the N-terminal helix. Therefore, binding of papiliocin to TLR4/MD-2 may be primarily mediated by electrostatic interactions with the amphipathic N-terminal helix. The flexible hinge region connecting the two helices may allow the recruitment of the hydrophobic carboxyl-terminal helix to the MD-2 protein to bind to the interface between TLR4 and MD-2.

Identification of Key Residues Required for Its Interaction with LPS. To investigate the key residues required for the interaction with LPS, we synthesized analogs of papiliocin by substituting positively charged residues with Glu (R1E, K3E, K6E, K7E, K10E, R13E, R16E, and K37E) and Glu with Arg (E9R), which are highly conserved in insect cecropins (*SI Appendix*, Fig. S3 *A* and *B*) and may form electrostatic interactions with LPS. We also substituted V28, V29, V35, and V36 in the hydrophobic carboxyl-terminal helix, as well as W2 and F5 with Ala. Antibacterial activities of these analogs were measured; we found that K3 and K6 dramatically decreased the antibacterial activity, indicating that they are key residues for the antibacterial activities of papiliocin, whereas substitution of R1, W2, F5, and R16 showed a two- to fourfold decrease in antibacterial activities (*SI Appendix*, Table S1). Interestingly, membrane depolarization of the intact *E. coli* cell, LAL assay, and ITC measurements showed that K3E and K6E completely lost membrane-depolarizing activities as well as LPS-binding properties, suggesting that K3 and K6 are key residues for interaction with LPS (*SI Appendix*, Fig. S7 *A–C*).

We further examined the anti-inflammatory activities and SEAP activities of K3E and K6E analogs in inhibiting TLR4 signaling, which are key residues for LPS binding of papiliocin (*SI Appendix*, Fig. S8 *A–D*). Compared to papiliocin, K3E and K6E

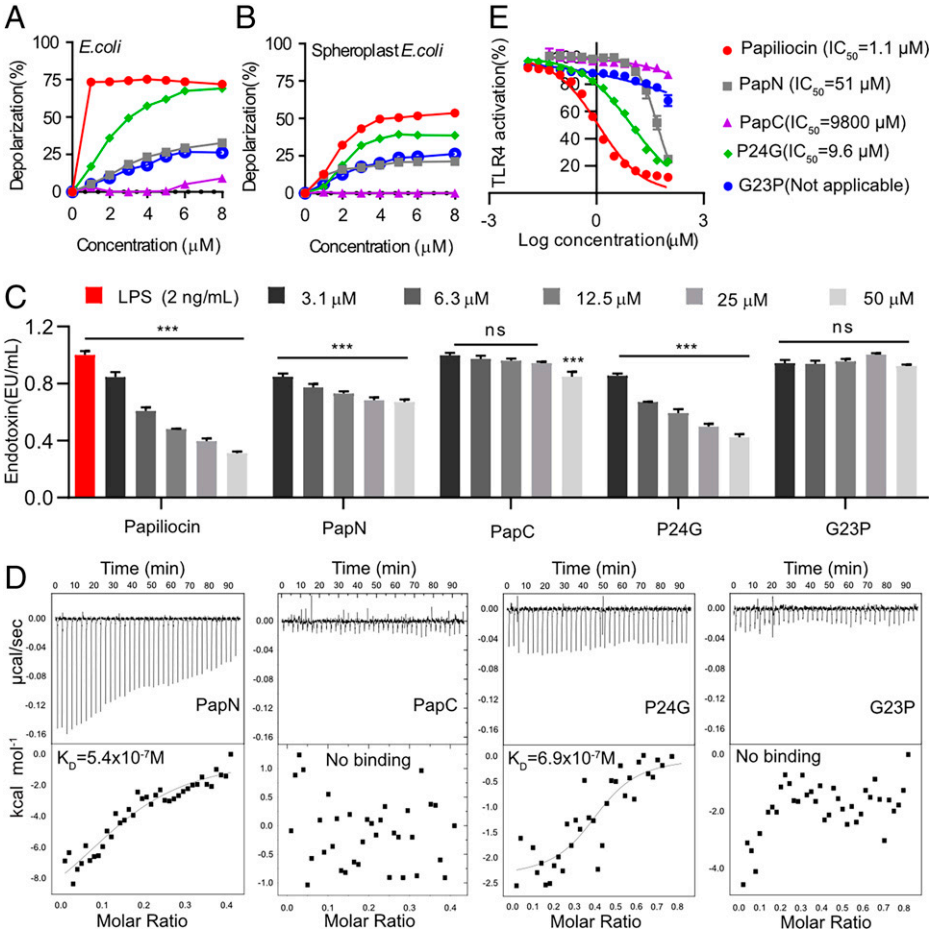

Fig. 3. Effect of important structural elements on LPS interactions of papiliocin. Concentration-dependent depolarization of (*A*) intact *E. coli* membrane and (*B*) *E. coli* spheroplasts by peptides (papiliocin, PapN, PapC, P24G, and G23P). (*C*) Effect of peptides on the regulation of TLR4 signaling as measured in SEAP assays. (*D*) LAL assay showing the LPS neutralization capacities of papiliocin and its analog (LPS, 2 ng/mL; peptides, 3.1, 6.3, 12.5, 25, and 50 μM). (*E*) ITC measurement showing the binding interaction of peptides (0.1 mM each) to 0.025 mM LPS. Upper panels represent the heat (μcal/s) of the injectant, and lower panels show the enthalpy (kcal/mol) of the injectant. The supplements show the binding affinity (K_D) of each interaction. Each bar represents the mean ± SEM of three independent experiments. ***$P < 0.001$, and ns, nonsignificant compared with control in two-way ANOVA with Dunnett's comparison test.

completely lost anti-inflammatory activities and SEAP activities, indicating that loss of the interaction of K3E or K6E with LPS affects the TLR4-inhibiting activities of K3E or K6E, as LPS clearance can be an alternative approach for suppressing TLR4 signaling.

Docking Model of Papiliocin and TLR4/MD-2. To better understand the detailed intermolecular interactions between papiliocin and TLR4/MD-2, a docking simulation was performed to construct a binding model using the crystal structure of TLR4/MD-2/LPS (41). On the basis of experimental data from the SEAP assay and binding energy, we selected the best binding model among 200 docking runs. The highest population among all clusters was observed for the docking model with the lowest binding energy (−7.476 kcal/mol). In this binding model, the carboxyl-terminal helix of papiliocin was buried deep within the β-sandwich hydrophobic pocket of MD-2, whereas the amphipathic N-terminal helix was bound to the interface between TLR4 and MD-2 (Fig. 2*D* and *SI Appendix*, Fig. S9*A*). Structural overlay of papiliocin in the docking model with the crystal structure of TLR4/MD-2/LPS (Fig. 2*D*) showed that the residues in TLR4 and MD-2 marked in red (*SI Appendix*, Fig. S9*B*) interacted with papiliocin in a manner similar to that required for LPS binding observed in the crystal structure of TLR4/MD-2/LPS (41). Similar to that observed for the hydrophobic acyl chains of LPS and other known antagonists such as eritoran and lipid IVA (41–43), numerous hydrogen bonds may form between TLR4 and the positively charged residues (R1, K6, R13, R16, and K21) in the N-terminal helix of papiliocin, which is consistent with the SPR data showing that PapN binds to TLR4/MD-2 and TLR4 with micromolar affinities. Surface representation in Fig. 2*E*, as well as detailed intermolecular interactions shown in Fig. 2*F*, clearly show that the hydrophobic side chains, V28, V29, A32, A33, V35, and V36 of the carboxyl-terminal helix of papiliocin, inserted into the hydrophobic pocket of MD-2, suggesting its role forming strong hydrophobic interactions with MD-2. Furthermore, hydrogen bonds were formed between K7 of papiliocin and S118 of MD-2 and between Q31 of papiliocin and K122 of MD-2, thereby mimicking the binding pattern of LPS to MD-2. In particular, the guanidino side chains of R13 and R16 at the N-terminal helix, which are highly conserved in insect cecropins, formed extensive hydrogen bonds with E321, G363, and G364 in the flexible loop region of TLR4, whereas LPS showed close contact with positively charged K362 and K341 in this loop region of TLR4 (Fig. 2*G*) (41). Furthermore, the positively charged side chain of R1 in papiliocin formed an electrostatic interaction with D294 of TLR4, which interacted with the inner core structure of LPS. Interestingly, the negatively charged side chain of E9 in papiliocin, which is highly

conserved in insect cecropins, formed ionic interactions with K341 and K362 of TLR4, which are important for binding of LPS to TLR4, as they interact with the phosphate groups in the lipid A structure of LPS (41). The W2 and F5 aromatic side chains of papiliocin further stabilized the binding by forming π-π stackings with Y295 and Y296 of TLR4, which is consistent with the STD effect (Fig. 2 *B*, *F*, and *G* and *SI Appendix*, Fig. S1*B*). These interactions between the N-terminal helix and TLR4/MD-2 interface may promote binding of the carboxyl-terminal hydrophobic helix to the MD-2 hydrophobic pocket and suppress TLR4-mediated signaling by inhibiting LPS binding to the TLR4/MD-2 complex, resulting in inhibition of TLR4/MD-2 dimerization. Thus, papiliocin may competitively prevent LPS binding to the TLR4/MD-2 complex as a potent antagonist of TLR signaling.

Identification of Key Residues Required for Interaction between Papiliocin and TLR4/MD-2. To validate our binding model, we synthesized analogs of papiliocin by substituting positively charged residues with Glu (R1E, R13E, and R16E) and by substituting E9 with Arg (E9R), which led to the formation of extensive electrostatic and hydrogen-bonding interactions with TLR4/MD-2 in the docking model (*SI Appendix*, Table S1). We also substituted V28, V29, V35, and V36 in the hydrophobic carboxyl-terminal helix, as well as W2 and F5, with alanine in the analogs (V28,29A, V35,36A, and W2F5A) to confirm the importance of the hydrophobic interactions. Except for V35 and V36, these residues are highly conserved in insect cecropins from the moth and butterfly (*SI Appendix*, Fig. S3*A*). Notably, all analogs showed weaker antibacterial activities against gram-negative bacteria, with R1E and R16E showing a much larger reduction in antibacterial activity compared to that of papiliocin, indicating the functional importance of these residues (*SI Appendix*, Table S1). E9R and W2F5A also reduced antibacterial effects by two- and fourfold, respectively. Furthermore, the inhibitory effects of all analogs on NO production in LPS-stimulated RAW 264.7 cells were much lower than those of papiliocin (Fig. 4*A*). Notably, R13E and R16E completely lost their anti-inflammatory effects (Fig. 4*A*), which agreed well with the binding model. W2, F5, and E9 also showed extensive interactions with TLR4 in the binding model (Fig. 2 *F* and *G*), and their amino-acid substitutions (W2F5A and E9R) showed a 25-fold decrease in SEAP activity (Fig. 4*B*). Compared to that of papiliocin, we observed a 27-fold decrease in the activities of V28,29A and a sixfold decrease in the activities of V35,36A. Unexpectedly, R16E completely lost the ability to inhibit TLR4 signaling, and R13E showed drastically weaker TLR4 inhibition (310-fold decrease) than papiliocin, implying that the highly conserved R13 and R16 are the key residues for TLR4/MD-2 interaction (Fig. 4*B*).

To determine whether these effects were an artifact of Glu substitution in R13E and R16E, we synthesized R13A and R16A by replacing Arg with Ala. Similar to those observed for R13E and R16E, the antibacterial, anti-inflammatory, and SEAP activities of R13A and R16A were significantly lower than those of papiliocin (*SI Appendix*, Table S1 and Fig. S10 *A*–*C*), confirming the importance of R13 and R16 in inhibiting TLR4 signaling.

R13 and R16 Are Key Residues of Papiliocin That Act as Competitive TLR4 Antagonists to LPS. Based on these results, we hypothesized that R13 and R16 regulate TLR4 signaling. Hence, we assessed the regulation of cell-surface expression of TLR4 by papiliocin and the R13E and R16E analogs using flow cytometry. Papiliocin pretreatment (blue) effectively inhibited LPS binding to RAW 264.7 cells, resulting in down-regulation of TLR4 expression (Fig. 4*C*). In contrast, R13E and R16E pretreatment did not inhibit LPS binding as well as surface expression of TLR4, similar to that observed in LPS-stimulated RAW 264.7 cells. To investigate whether papiliocin, R13E, and R16E competitively regulate LPS, we examined the posttreatment scores (LPS simulation followed by peptide treatment). We found that papiliocin (green) caused competitive replacement of prebound LPS to TLR4 receptors and restricted LPS attachment to the TLR4 receptor, while R13E and R16E posttreatment did not replace prebound LPS on the RAW 264.7 cell surface; thus, attached LPS rapidly activated TLR4 expression, similar to that in LPS-stimulated RAW 264.7 cells (Fig. 4*C*). In our binding model, the guanidino side chains of R13 or R16 in papiliocin formed extensive hydrogen bonds with E321, G363, and G364 (Fig. 2 *F* and *G*). Thus, R13E and R16E may not interact strongly with the interface of TLR4 and MD-2, supporting our docking model. These results suggest that R13 and R16 are the key papiliocin residues acting as competitive TLR4 antagonists of LPS, highlighting alternative approaches for combating postsepsis syndrome.

R13E and R16E were maintained binding affinity to LPS but lost their TLR4-inhibiting abilities, we suggest that R13 and R16 at the middle of the PapN amphiphatic helix, along with the flexible hinge region, may play important roles in TLR4/MD2 binding. In contrast, K3 and K6 at the N terminus of the PapN helix, along with the flexible hinge region, may play critical roles in LPS binding.

Papiliocin Is a Potent and Safer Peptide Antibiotic with Lower Nephrotoxicity Compared to PMB. Next, we investigated the potency of papiliocin as a safe and effective antibiotic against carbapenem-resistant gram-negative infection and compared it with that of PMB. Papiliocin displayed higher antibacterial activities against all carbapenem-resistant bacteria such as CREC, carbapenem-resistant *K. pneumoniae*, and carbapenem-resistant *A. baumannii* than PMB and melittin; however, papiliocin and PMB did not effectively inhibit gram-positive bacteria (*SI Appendix*, Table S2). Notably, CREC, carbapenem-resistant *K. pneumoniae*, and carbapenem-resistant *A. baumannii* were susceptible to papiliocin, whereas imipenem and meropenem failed to show bactericidal effects against any carbapenem-resistant bacteria. Furthermore, 1 μM papiliocin killed *E. coli* and CREC more rapidly in a time-dependent manner than PMB (*SI Appendix*, Fig. S11 *A* and *B*). Antibiotic resistance also enhances biofilm-associated infections, further increasing the risk of bacterial dissemination in clinical practice (44). Papiliocin inhibited the biofilm development of carbapenem-resistant bacteria more effectively than PMB and other antibiotics (*SI Appendix*, Fig. S11*C*).

Morphological changes in *E. coli* after incubation with 2 μM papiliocin for up to 4 h were observed using field-emission scanning electron microscopy (FE-SEM) and field-emission transmission electron microscopy (FE-TEM) (*SI Appendix*, Fig. S11*D*). After papiliocin treatment, *E. coli* cells exhibited large cavities and cell shrinkage even after 1 h. FE-TEM observations showed that papiliocin induced the release of cytoplasmic contents after 1 h and that of small and large vesicles with severe clustering of DNA and ribosomes after 2 h and complete cellular damage and release of intracellular contents after 4 h. These results (*SI Appendix*, Fig. S11 *A*–*D* and Table S2) confirmed that the bactericidal activities of papiliocin were comparable or superior to that of PMB and that it acted via membrane permeabilization.

To examine the safety of papiliocin versus that of PMB, we first analyzed the toxic effects of these molecules toward RAW 264.7 cells. The results showed that treatment with papiliocin led to 100% and 78.0% cell survival rates at 50 μM and 100 μM, whereas PMB led to only 30.6% and 15.5% cell survival at 50 μM and 100 μM, respectively (*SI Appendix*, Fig. S12*A*), indicating that papiliocin was considerably less toxic to

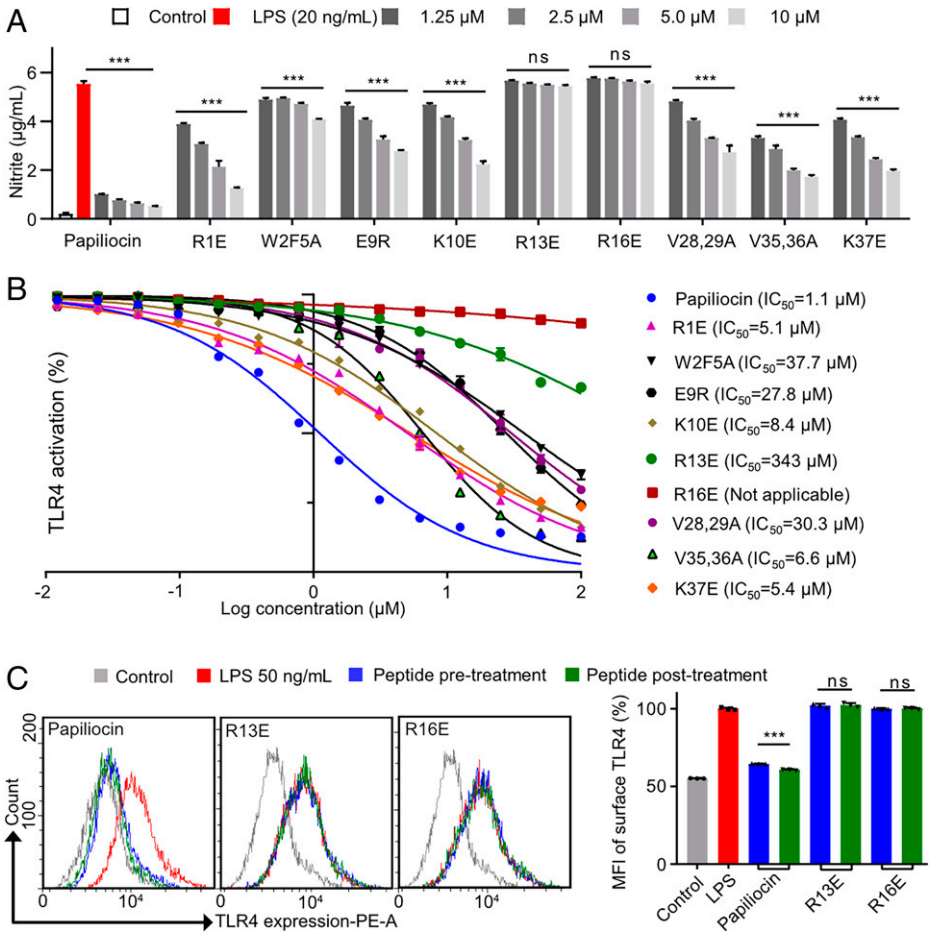

Fig. 4. R13 and R16 are the key residues contributing to the TLR4 antagonistic activity of papiliocin. (*A*) Effects of papiliocin analogs on (*A*) nitrite inhibition in RAW 264.7 cells stimulated with LPS (LPS, 20 ng/mL; peptides, 1.25, 2.5, 5.0, and 10 μM) and (*B*) TLR4 inactivation as measured by SEAP assays in LPS-stimulated HEK-BlueTM hTLR4 cells (peptides, 0 to 100 μM). (*C*) Flow cytometry analysis showing the effect of papiliocin and its specific analogs on inhibition of LPS-stimulated TLR4 receptor expression in RAW 264.7 cells. Bar graph indicating the MFI of TLR4 surface protein expression (%) as measured by flow cytometry. RAW 264.7 cells pretreated with 10 μM peptides (papiliocin, R13E, andR16E) were indicated in blue, posttreated in green, or in red when 50 ng/mL LPS was added , and the expressions were analyzed at 24 h. Each bar represents mean ± SEM of three independent experiments. IC_{50} by nonlinear regression analysis (*B*), ***$P < 0.001$, and ns, nonsignificant compared with LPS control by one-way ANOVA with Dunnett's comparison test (*A* and *C*).

RAW 264.7 cells than PMB. As PMB is known to cause severe nephrotoxicity in clinical settings, we next analyzed acute nephrotoxicity by administrating low (5 mg/kg/day for 5 d) and high (20 mg/kg twice per day for 3 d) doses of both peptides to mice. When 20 mg/kg PMB was injected twice per day for 3 d, serum creatinine and blood urea nitrogen (BUN) levels were elevated by 37.1% and 26.6%, respectively, indicating that PMB has severe nephrotoxicity (Fig. 5*A* and *SI Appendix*, Fig. S12*B*). In contrast, compared to the control, neither lower dose of PMB nor any dose of papiliocin induced any aberrant changes in creatine level. Similarly, the levels of the liver enzymes, aspartate transaminase (AST) and alanine aminotransferase (ALT), increased by 17.8% and 30.6%, respectively, in mice challenged only with PMB (20 mg/kg) (*SI Appendix*, Fig. S12*B*), confirming the nonhepatotoxic effect of papiliocin. In addition, PMB-treated mice (20 mg/kg, two doses for 3 d) showed notable kidney damage such as vascular congestion and tubular degeneration associated with focal necrosis in tubular epithelial cells, whereas papiliocin treatment did not show any signs of morphology changes in the kidneys, similar to that of control mice (*SI Appendix*, Fig. S12*C*). These results indicate that papiliocin is a potent and safer peptide antibiotic with lower nephrotoxicity compared to PMB.

Papiliocin Acted as a Potent Antiseptic Peptide in an In Vivo *E. coli* K1–Induced Sepsis Model. We assessed the antiseptic potential of papiliocin using an *E. coli* K1–infected mouse model of sepsis and compared it to that of PMB. Survival analysis (Fig. 5*B*) showed that mice challenged with *E. coli* K1 (5×10^7 colony-forming units [CFU]/mouse) exhibited 100% mortality after 12 h of infection. Papiliocin (10 mg/kg) protected mice from *E. coli* K1 infection, as manifested by a survival rate of 84.0%, whereas 10 mg/kg PMB resulted in a 78.0% survival rate for up to 96 h. In the sepsis model, treatment with papiliocin (1 mg/kg) after *E. coli* K1 infection significantly reduced the total bacterial load in visceral organs compared to PMB-treated and untreated *E. coli* K1–infected mice (Fig. 5*C*). Notably, papiliocin and PMB treatment significantly reduced endotoxin levels by 35.9% and 34.6%, respectively, indicating that the in vivo endotoxin removal capacities of papiliocin and PMB were comparable (Fig. 5*D*).

In addition, the serum and lung tissue levels of TNF-α and IL-6 were significantly reduced in both papiliocin- and PMB-treated mice compared to those in *E. coli* K1–infected control mice (Fig. 5 *E*–*H*). Papiliocin treatment effectively reduced ALT, AST, and BUN levels to 28.0%, 26.9%, and 24.5%, respectively, whereas PMB treatment reduced them to 19.4%, 25.7%, and 16.7%,

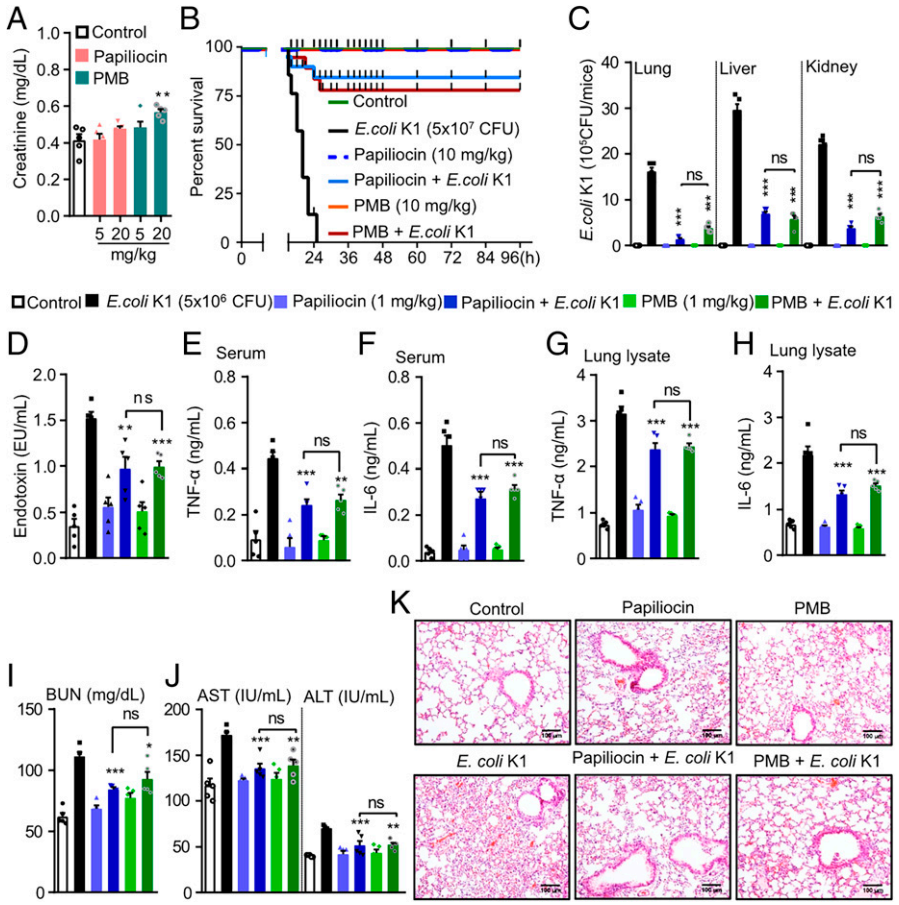

Fig. 5. Antiseptic effects of papiliocin and PMB in the *E. coli* K1–induced sepsis mouse model. (*A*) Effect of papiliocin and PMB on systemic toxic markers (creatinine) using ICR mice. Mice (n = 5 per group) were i.p. injected with papiliocin or PMB (5 mg/kg/day for 5 d and 20 mg/kg twice a day for 3 d). (*B*) Papiliocin shows improved survival rates of mice infected by *E. coli* K1 compared to PMB. Mice (n = 20 per group) were i.p. injected with papiliocin or PMB (10 mg/kg) 1 h before i.p. injection of *E. coli* K1 (5×10^7 CFU/mouse), and survival was observed during the next 96 h. (*C*) Papiliocin effectively clearing the bacterial colonization in the liver, lung, and kidney lysates of *E. coli* K1 spesis mice. Mice (n = 5 mice per group) were administered 1 mg/kg peptides 1 h before injection of *E. coli* K1 (5×10^6 CFU/mouse), and analyses were performed 16 h later. (*D*) Papiliocin and PMB sensitize the circulating *E. coli* K1 endotoxin for degradation in mice. (*E–H*) Papiliocin and PMB modulate the cytokine levels (TNF-α and IL-6) in the serum and lung lysates of *E. coli* K1–infected mice. (*I* and *J*) Serum levels of BUN, AST, and ALT. (*K*) Hematoxylin and eosin–stained lung sections show the effect of papiliocin and PMB on neutrophil infiltration (magnification 20×). (Scale bar, 100 μm.) Each bar represents mean ± SEM of three independent experiments. $^{**}P < 0.01$, $^{***}P < 0.001$, and ns, nonsignificant compared with control by one-way ANOVA with Dunnett's comparison test (*A* and *C–J*) and Kaplan–Meyer test (*B*).

respectively, indicating the effective antiseptic potential of papiliocin (Fig. 5 *I* and *J*). Furthermore, lung tissue histology revealed that papiliocin and PMB treatment significantly protected against lung damage in the *E. coli* K1–infected group in response to high levels of infiltrating polymorphonuclear neutrophils (Fig. 5*K*). Taken together, our results confirmed that papiliocin can be used as a starting point to develop a potent alternative to PMB for treating gram-negative sepsis with lower toxicity.

Discussion

In this study, we aimed to decipher the molecular mechanism underlying TLR4 antagonistic and antiseptic activities of papiliocin and to understand the related mechanism operating in insect innate immune response to microbial infection. Recognition of LPS on the outer membrane of gram-negative bacteria by TLR4 triggers the overproduction of uncontrolled inflammatory cytokines, which can ultimately lead to sepsis and septic shock. Extensive research has demonstrated that AMPs can antagonize LPS (45). For example, mammalian cathelicidins, such as LL-37 and CRAMP, showed anti-inflammatory activities and reduced TLR4 activation via LPS neutralization (46, 47). PMB is a well-known LPS-neutralizing peptide that inhibits the inflammatory effects of LPS via binding to lipid A, enhancing the membrane permeability of gram-negative bacteria. Currently, the continuous emergence and evolution of carbapenem-resistant bacteria pose a serious clinical challenge, which has led to the revival of previously used drugs such as PMB despite its known toxicities (48). In this study, papiliocin showed potent LPS-neutralizing activity, with a binding affinity of 6.3×10^{-8} M to LPS, which was superior to that of PMB (3.3×10^{-7} M). In addition, we proposed a mechanism for the bactericidal effect of papiliocin, in which it killed *E. coli* by permeabilizing its membrane via direct interaction with LPS. The bactericidal activity of papiliocin against CREC was superior to that of PMB, demonstrated by MIC measurements, time-dependent killing assays, and biofilm inhibition. As LPS binding is critical for the immunomodulatory properties of papiliocin, our flow cytometry data revealed that papiliocin has a dual mode of action, including a direct binding interaction with LPS, as well as replacement of prebound LPS following binding with their receptors, which down-regulates the receptor pathway for immune inactivation. Residual analysis of the LPS interaction indicated that positively charged residues, such as K3 and K6 near the N terminus, which are highly conserved in insect cecropins, along with the flexible hinge region, play essential roles in antibacterial activity and LPS interaction.

Binding to the LPS of gram-negative bacteria mediates TLR4/MD-2 complex dimerization, resulting in systemic inflammatory cascades and septic shock. Unfortunately, the available TLR4 antagonists were not successful in clinical trials (8, 9). Eritoran, a synthetic antagonist of TLR4, mimics the structure of LPS lipid A and targets the MD-2 hydrophobic pocket to inhibit the TLR4/MD-2 interaction (42, 49). FP7, a lipid X mimetic, was developed based on the chemical structure of a diacylated diphosphorylated monosaccharide to target MD-2 (50). Peptide inhibitors have been developed as potential antagonists against TLR4-MD2, too (51, 52). In contrast, TAK-242 (resatorvid) specifically inhibits TLR4 signaling by binding to the intracellular domain of TLR4 and disrupting the interaction of TLR4 with adaptor proteins (53). However, both eritoran and TAK-242 failed in phase III clinical trials because of safety and efficacy issues. Therefore, we next analyzed the TLR4 regulatory effects of papiliocin in cell-based and non–cell-based assays. We demonstrated that papiliocin specifically targeted TLR4 (IC_{50} = 1.1 μM) with micromolar binding affinity and down-regulated the TLR4 inflammatory pathway, indicating that it can be a potent antagonist of TLR4. Importantly, our flow cytometry data confirmed that with pretreatment, papiliocin effectively bound to the macrophage surface and prevented LPS binding, thereby inhibiting TLR4 expression. Interestingly, after treatment, antagonist papiliocin competitively replaced prebound LPS from the cell surface and reduced TLR4 expression, indicating that papiliocin inhibits TLR4-mediated signaling by competing with LPS.

Since circumstantial evidence linking the dose-limiting nephrotoxicity of PMB limits its use in clinical applications, there are emerging needs to develop safe alternative (48). In this study, papiliocin treatment in the *E. coli* septic shock mouse model significantly reduced the bacterial load in visceral organs and reduced proinflammatory cytokine secretion, suggesting its potent therapeutic efficacy against gram-negative sepsis with considerably lower nephrotoxicity than PMB. Furthermore, we elucidated a dual mechanism underlying the antiseptic activities of papiliocin. First, papiliocin binds directly to LPS released from the outer membrane of gram-negative bacteria, resulting in LPS clearance during sepsis. Second, papiliocin showed efficacy against gram-negative sepsis via competitive inhibition of LPS binding to TLR4 by directly binding to TLR4/MD-2.

Extensive research has revealed that the insect immune system responds to infections by activating genes encoding potent AMPs (23). Notably, Toll and immune-deficiency pathways are the major regulators of AMPs in insects, suggesting that humoral immunity may be involved in the clearance of the bacterial burden (54). In *D. melanogaster*, proteoglycans activate AMP gene expression; however, LPS activates neither the immune-deficiency pathway nor the Toll pathway in *Drosophila* (55). In contrast, in *B. mori*, LPS from gram-negative infection can activate the expression of AMPs such as cecropin B, whereas in mammals, TLR4 requires MD-2 for LPS recognition in response to gram-negative infections (20, 27). Recently, *B. mori* Toll9 was found to colocalize with BmMD-2A and BmMD-2B on the surface of *B. mori* immune tissues (21). Simulated structures of *B. mori* MD-2A–lipid A and ML-2B–lipid A complexes based on the structure of the human MD2–lipid A complex revealed that similar to human MD-2, BmMD-2A and BmMD-2B contain two antiparallel β-sheets and a deep hydrophobic cavity. The hydrophobic acyl chains of lipid A can bind to the human MD-2/LPS complex in this cavity, albeit in different directions, implying that *B. mori* MD-2–like proteins are the accessary proteins required for LPS recognition (20). Similar to mammalian TLR4 ectodomains, the homology-modeled structure of *B. mori* Toll9 using human TLR4 as a template contains a cysteine cluster carboxyl terminus to the leucine-rich repeats, with a characteristic horseshoe-like shape, suggesting that insect Toll9 evolutionarily clusters with mammalian TLR4 (21). The LPS recognition and signaling functions of the Toll9/MD-2–like protein complex of *B. mori* may be similar to that of the mammalian TLR4/MD-2 complex (21). As shown in *SI Appendix*, Fig. S3, the sequences of insect cecropins from the moth and butterfly, including papiliocin, were >90% similar (*SI Appendix*, Fig. S3*A*), whereas papiliocin showed relatively lower sequence homology with cecropins from *D. melanogaster* (*SI Appendix*, Fig. S3*B*), supporting their findings.

Among AMPs, cecropins play important roles in the innate immune response of insects against invading pathogens and show high sequence homology with each other (23). Therefore, we hypothesized that specific amino-acid residues and structural elements perform immune regulatory function and specifically interact with TLR4/MD-2, thereby abolishing LPS signal transduction. We also predicted that these structural aspects may play important roles in Toll9-mediated insect immune response, particularly in the moth and butterfly. Therefore, to improve our understanding of the structural elements, as well as key residues required for the TLR4 antagonistic activity of papiliocin, binding measurements, docking simulations, and in vitro assays for various analogs were performed. Amphipathic N-terminal helices are involved in extensive interactions with the interface between TLR4 and MD-2, and the flexibility of the hinge region is essential for recruiting the binding of the conserved hydrophobic carboxyl-terminal helix to the hydrophobic pocket of MD-2. Notably, cell-based analysis confirmed that R13E and R16E analogs neither show competitive regulation nor affect LPS-stimulated TLR4 expression in RAW 264.7 cells, suggesting that these residues in papiliocin play key roles in the competitive regulation of TLR4. Strong electrostatic interactions of R13 and R16 promoted binding of the N-terminal helix of papiliocin to the interface of TLR4 and MD-2 and that of the hydrophobic carboxyl-terminal helix to the MD-2 pocket, which allowed papiliocin to compete with LPS for TLR4/MD-2 binding and possibly suppressed LPS-induced TLR4/MD-2 dimerization during infection by gram-negative bacteria.

Interestingly, R1, W2, F5, E9, R13, and R16 in the N-terminal helix of papiliocin, which formed extensive electrostatic and hydrophobic interactions between TLR4 and MD-2 in the docking model, are completely conserved in *B. mori* cecropin A and B. Furthermore, alanine, valine, and hydrophobic residues in the hydrophobic carboxyl-terminal helix are highly conserved in insect cecropins from different species, indicating that they are involved in similar hydrophobic interactions with hydrophobic pockets of MD-2. Therefore, the interactions between papiliocin and human TLR4/MD-2 observed in this study may be functionally and evolutionarily related to the interactions between insect cecropins and Toll9/MD-2–like proteins, which are essential for insect innate immunity after microbial infection. All interactions observed between papiliocin and TLR4/MD-2 may mimic the interactions between B. mori cecropins and Toll9/MD-2 proteins, which are essential for insect immune response. However, as the X-ray structure of TLR4/MD-2 in complex with papiliocin could not be determined, the interacting residues between these molecules remain unknown and require further investigation.

In conclusion, we showed that the human TLR4 antagonizing ability of papiliocin may be highly similar to its activity as an innate immune molecule involved in the immune response of insects to bacterial infection. This study also highlights the potential of using papiliocin to develop potent TLR4 peptide antagonists that can be used to treat gram-negative sepsis.

Materials and Methods

A full description of the following methods for the data is shown in *SI Appendix, Supplementary Materials and Methods*: Bacterial strains,

antimicrobial activity, depolarization, time-killing assay, antibiofilm assay, electron microscopy, LPS neutralization, BC displacement assay, ITC, SEAP activity, enzyme-linked immunosorbent assay (ELISA), STD NMR experiment, SPR measurement, docking simulation, and in vitro and in vivo toxicity.

Peptide Synthesis. Peptides were synthesized by solid-phase synthesis using *N*-(9-fluorenyl) methoxycarbonyl and were purified with over 98% purity by reversed-phase preparative high-performance liquid chromatography, and molecular masses were confirmed by Anygen Co., Ltd.

Flow Cytometry. The binding of peptides to FITC-conjugated LPS from *E. coli* 055:B5 (Sigma-Aldrich) was analyzed using Cytoflex flow cytometry (Beckman Coulter). RAW 264.7 cells (10^6) were incubated with peptides (40 μM) or FITC-LPS (40 μg/mL) under serum-free conditions for 30 min at 4 °C and washed with phosphate buffered saline (PBS), and the fluorescence intensity of the cell suspensions was analyzed using flow cytometry. Similarly, RAW 264.7 cells (10^6) were pre- and posttreated each with 10 μM peptides (Papiliocin, R13E, and R16E) or LPS (50 ng/mL) for 30 min and then incubated for 24 h. Cells (10^6) were blocked with 1% bovine serum albumin (BSA; Thermo Fisher Scientific) for 20 min at 4 °C followed by incubation with TLR4 antibody (Abcam, No. ab13556, 0.5 μg/106 cells) for another 20 min (4 °C). The cells were washed with ice-cold PBS and incubated with Alexa Fluor 546–conjugated secondary antibody (Invitrogen, No. A-10040, 1:200 dilution) for 20 min. After the PBS wash, the cells were analyzed using flow cytometry (Beckman Coulter).

Specificity of Papiliocin against Various TLRs. To determine the regulatory effect of papiliocin on the nitric oxide production induced by various TLRs, we analyzed them as previously discribed with various TLR-specific agonists such as Pam_3CSK_4 (TLR1/2, 100 ng/mL), Pam_2CSK_4 (TLR2/6, 100 ng/mL), polyinosinic–polycytidylic acid (Poly(I:C)) (TLR3, 3 μg/mL), LPS (TLR4, 20 ng/mL), imiquimod (TLR7, 1 μg/mL), and ODN1826 (TLR9, 30 μg/mL). These were purchased from Invivogen (San Diego). RAW 264.7 cells were pretreated with papiliocin (0 to 5 μM) for 1 h and then stimulated with the TLR agonists. After 16 h, Griess reagent was used to measure the NO production.

Immunofluorescence Analysis. The 5×10^5 RAW 264.7 cells were seeded on the coverslips in 6-well plates. After 16 h, cells were pretreated with 10 μM papiliocin for 1 h before 50 ng/mL LPS treatment. After 30 min, the cells were fixed by 4% paraformaldehyde and permeabilized by 0.3% Triton X-100. After blocking (5% BSA), primary antibodies against p-NF-κB (Cell Signaling Technology, No. 3031, 1:50) or α-tubulin (Cell Signaling Technology, No. 3873, 1:200) were added for 90 min and then incubated with Alexa Fluor 488 (Invitrogen, No. A-28175) or Alexa Fluor 546 (Invitrogen, No. A-10040, 1:200) conjugated secondary antibodies for 40 min. We counterstained the nuclear region using Hoechst 33258 (Invitrogen, No. H3569, 1:200) and visualized by fluorescence microscope (BX61-32FDIC, Olympus) and analyzed by the MetaMorph Image analysis program (Molecular Devices).

Western Blotting. Total proteins of all cell lysates were extracted using radio immunoprecipitation buffer (RIPA, Sigma-Aldrich). The cytoplasmic and nuclear protein fractions were extracted using an NE-PER Nuclear and Cytoplasmic Extraction Reagents kit (Thermo Fisher Scientific). Protein concentrations were measured using a BCA protein assay kit (Thermo Fisher Scientific), electroblotted to polyvinylidene fluoride membrane, and subsequently incubated with primary antibodies specific for MyD88 (Abcam, No. ab2064, 1:1,000), p-TAK1 (Abcam, No. ab109404, 1:1,000), total-ERK (Cell Signaling Technology, No. 9107, 1:1,000), p-ERK (Cell Signaling Technology, No. 9106, 1:1,000), total-JNK (Cell Signaling Technology, No. 9252, 1:1,000), p-JNK (Cell Signaling Technology, No. 4671, 1:1,000), total-p38 (Cell Signaling Technology, No. 9212, 1:1,000), p-p38 (Cell Signaling Technology, No. 9211, 1:1,000), total- NF-κB (Cell Signaling Technology, No. 9609, 1:1,000), p-NF-κB, and β-actin (Santa Cruz Biotechnology, No. sc-47778, 1:1,000). After incubation with peroxidase-conjugated secondary antibodies, protein complexes were visualized by WestGlowTM Chemiluminescent Substrate (Biomax Co., Ltd). The relative band intensities were quantified using the ImageJ software (version 1.52, NIH).

Animals. Female mice from the ICR (Institute of Cancer Research) were background purchased from Orient and were housed under a specific pathogen-free and humidity-controlled environment. All procedures were reviewed and approved by the Institutional Animal Care and Use Committee (IACUC) of Konkuk University, South Korea (IACUC No.: KU20192). This has been used to determine the in vivo toxicities of peptides (*SI Appendix*).

Survival Analysis. ICR mice were divided into six groups (20 mice per group). Mice were treated with an intraperitoneal (i.p.) injection of PBS (control group), a 10-fold increment of gram-negative *E. coli* K1 (5×10^7 CFU/mouse, American Type Culture Collection [ATCC] 700973), peptide control papiliocin, or PMB (10 mg/kg). Treated mice received papiliocin or PMB 1 h before *E. coli* K1 injection. The survival was examined at 3-h intervals for 96 h.

***E. coli* K1 Sepsis Mouse Model.** ICR mice were randomly divided in to six groups (5 mice per group). PBS alone served as the vehicle. Peptide control mice received i.p. injections of papiliocin or PMB (1 mg/kg in PBS). For peptide treatment groups, papiliocin or PMB (1 mg/kg) was i.p. injected 1 h before *E. coli* K1 injection (5×10^6 CFU/mice). At the time of killing, the lungs, liver, and kidneys were removed aseptically and were then homogenized using ice-cold PBS. To assess the relative abundance of *E. coli*, all homogenates (1:1,000, PBS) were plated onto Luria–Bertani agar, and the numbers of bacteria colonies were counted (56). The levels of inflammatory cytokines (TNF-α and IL-6) were measured in the serum and lung lysates using corresponding ELISA kits (R&D Systems). The contents of AST, ALT, and BUN were determined using a standard kit from Asan Pharmaceutical, as described previously (37). To estimate polymorphonuclear leukocyte (PMN) infiltration levels, 4-μm-thick sections were prepared from paraffin-blocked lungs and sequentially processed for hematoxylin and eosin staining and examined using a light microscope.

Statistical Analysis. All analyses were repeated at least three times using independent experiments (mean ± SEM). Data were analyzed by nonlinear regression analysis, Kaplan–Meier log-rank test, one-way ANOVA, and two-way ANOVA followed by Dunnett's tests using GraphPad Prism (GraphPad Software Inc.).

Data Availability. All study data are included in the article and/or supporting information.

ACKNOWLEDGMENTS. This work was supported by a National Research Foundation of Korea grant funded by the Korean government (Ministry of Science and Information and Communication Technology [MSIT]) (No. 2020R1A2C2005338).

1. K. Takeda, S. Akira, Toll-like receptors in innate immunity. *Int. Immunol.* **17**, 1–14 (2005).
2. Y. C. Lu, W. C. Yeh, P. S. Ohashi, LPS/TLR4 signal transduction pathway. *Cytokine* **42**, 145–151 (2008).
3. A. Ciesielska, M. Matyjek, K. Kwiatkowska, TLR4 and CD14 trafficking and its influence on LPS-induced pro-inflammatory signaling. *Cell. Mol. Life Sci.* **78**, 1233–1261 (2021).
4. A. Pop-Vicas, S. M. Opal, The clinical impact of multidrug-resistant gram-negative bacilli in the management of septic shock. *Virulence* **5**, 206–212 (2014).
5. M. Bassetti, A. Vena, C. Sepulcri, D. R. Giacobbe, M. Peghin, Treatment of bloodstream infections due to Gram-negative bacteria with difficult-to-treat resistance. *Antibiotics (Basel)* **9**, 632 (2020).
6. G. V. Asokan, T. Ramadhan, E. Ahmed, H. Sanad, WHO global priority pathogens list: A bibliometric analysis of Medline-Pubmed for knowledge mobilization to infection prevention and control practices in Bahrain. *Oman Med. J.* **34**, 184–193 (2019).
7. J. D. Lutgring, Carbapenem-resistant Enterobacteriaceae: An emerging bacterial threat. *Semin. Diagn. Pathol.* **36**, 182–186 (2019).
8. W. Gao, Y. Xiong, Q. Li, H. Yang, Inhibition of toll-like receptor signaling as a promising therapy for inflammatory diseases: A journey from molecular to nano therapeutics. *Front. Physiol.* **8**, 508 (2017).
9. S. Federico *et al.*, Modulation of the innate immune response by targeting toll-like receptors: A perspective on their agonists and antagonists. *J. Med. Chem.* **63**, 13466–13513 (2020).
10. A. Romerio, F. Peri, Increasing the chemical variety of small-molecule-based TLR4 modulators: An overview. *Front. Immunol.* **11**, 1210 (2020).
11. M. Zasloff, Antimicrobial peptides of multicellular organisms. *Nature* **415**, 389–395 (2002).
12. K. A. Brogden, Antimicrobial peptides: Pore formers or metabolic inhibitors in bacteria? *Nat. Rev. Microbiol.* **3**, 238–250 (2005).
13. G. Diamond, N. Beckloff, A. Weinberg, K. O. Kisich, The roles of antimicrobial peptides in innate host defense. *Curr. Pharm. Des.* **15**, 2377–2392 (2009).
14. J. Mwangi *et al.*, The antimicrobial peptide ZY4 combats multidrug-resistant *Pseudomonas aeruginosa* and *Acinetobacter baumannii* infection. *Proc. Natl. Acad. Sci. U.S.A.* **116**, 26516–26522 (2019).
15. T. Velkov, K. D. Roberts, R. L. Nation, P. E. Thompson, J. Li, Pharmacology of polymyxins: New insights into an 'old' class of antibiotics. *Future Microbiol.* **8**, 711–724 (2013).
16. S. C. Nang, M. A. K. Azad, T. Velkov, Q. T. Zhou, J. Li, Rescuing the last-line polymyxins: Achievements and challenges. *Pharmacol. Rev.* **73**, 679–728 (2021).
17. Q. Wu, J. Patočka, K. Kuča, Insect antimicrobial peptides, a mini review. *Toxins (Basel)* **10**, 461 (2018).

18. K. V. Anderson, G. Jürgens, C. Nüsslein-Volhard, Establishment of dorsal-ventral polarity in the Drosophila embryo: Genetic studies on the role of the Toll gene product. *Cell* **42**, 779–789 (1985).
19. B. Lemaitre, J. Hoffmann, The host defense of *Drosophila melanogaster*. *Annu. Rev. Immunol.* **25**, 697–743 (2007).
20. R. N. Zhang *et al.*, An ML protein from the silkworm *Bombyx mori* may function as a key accessory protein for lipopolysaccharide signaling. *Dev. Comp. Immunol.* **88**, 94–103 (2018).
21. R. Zhang *et al.*, Toll9 from *Bombyx mori* functions as a pattern recognition receptor that shares features with Toll-like receptor 4 from mammals. *Proc. Natl. Acad. Sci. U.S.A.* **118**, e2103021118 (2021).
22. S. Cociancich, P. Bulet, C. Hetru, J. A. Hoffmann, The inducible antibacterial peptides of insects. *Parasitol. Today* **10**, 132–139 (1994).
23. D. Brady, A. Grapputo, O. Romoli, F. Sandrelli, Insect cecropins, antimicrobial peptides with potential therapeutic applications. *Int. J. Mol. Sci.* **20**, 5862 (2019).
24. J. L. Imler, P. Bulet, Antimicrobial peptides in Drosophila: Structures, activities and gene regulation. *Chem. Immunol. Allergy* **86**, 1–21 (2005).
25. H. Steiner, D. Hultmark, A. Engström, H. Bennich, H. G. Boman, Sequence and specificity of two antibacterial proteins involved in insect immunity. *Nature* **292**, 246–248 (1981).
26. I. Morishima, S. Suginaka, T. Ueno, H. Hirano, Isolation and structure of cecropins, inducible antibacterial peptides, from the silkworm, *Bombyx mori*. *Comp. Biochem. Physiol. B* **95**, 551–554 (1990).
27. H. Tanaka *et al.*, Lipopolysaccharide elicits expression of immune-related genes in the silkworm, Bombyx mori. *Insect Mol. Biol.* **18**, 71–75 (2009).
28. A. Giacometti *et al.*, Effect of mono-dose intraperitoneal cecropins in experimental septic shock. *Crit. Care Med.* **29**, 1666–1669 (2001).
29. L. Wei *et al.*, Anti-inflammatory activities of Aedes aegypti cecropins and their protection against murine endotoxin shock. *Parasit. Vectors* **11**, 470 (2018).
30. O. Romoli *et al.*, Enhanced silkworm Cecropin B antimicrobial activity against *Pseudomonas aeruginosa* from single amino acid variation. *ACS Infect. Dis.* **5**, 1200–1213 (2019).
31. E. Lee *et al.*, Structure-activity relationships of cecropin-like peptides and their interactions with phospholipid membrane. *BMB Rep.* **46**, 282–287 (2013).
32. S. R. Kim *et al.*, Characterization and cDNA cloning of a cecropin-like antimicrobial peptide, papiliocin, from the swallowtail butterfly, *Papilio xuthus*. *Mol. Cells* **29**, 419–423 (2010).
33. J. K. Kim *et al.*, Structure and function of papiliocin with antimicrobial and anti-inflammatory activities isolated from the swallowtail butterfly, *Papilio xuthus*. *J. Biol. Chem.* **286**, 41296–41311 (2011).
34. E. Lee *et al.*, Functional roles of aromatic residues and helices of papiliocin in its antimicrobial and anti-inflammatory activities. *Sci. Rep.* **5**, 12048 (2015).
35. P. Durai, Y. Lee, J. Kim, D. Jeon, Y. Kim, Biophysical studies reveal key interactions between papiliocin-derived PapN and lipopolysaccharide in Gram-negative bacteria. *J. Microbiol. Biotechnol.* **28**, 671–678 (2018).
36. A. Shin *et al.*, Peptoid-substituted hybrid antimicrobial peptide derived from papiliocin and magainin 2 with enhanced bacterial selectivity and anti-inflammatory activity. *Biochemistry* **54**, 3921–3931 (2015).
37. J. Kim *et al.*, Development of a novel short 12-meric papiliocin-derived peptide that is effective against Gram-negative sepsis. *Sci. Rep.* **9**, 3817 (2019).
38. M. Piazza *et al.*, Evidence of a specific interaction between new synthetic antisepsis agents and CD14. *Biochemistry* **48**, 12337–12344 (2009).
39. H. J. Shin *et al.*, Kinetics of binding of LPS to recombinant CD14, TLR4, and MD-2 proteins. *Mol. Cells* **24**, 119–124 (2007).
40. X. Cheng, J. K. Kim, Y. Kim, J. U. Bowie, W. Im, Molecular dynamics simulation strategies for protein-micelle complexes. *Biochim. Biophys. Acta* **1858** (7 Pt B), 1566–1572 (2016).
41. B. S. Park *et al.*, The structural basis of lipopolysaccharide recognition by the TLR4-MD-2 complex. *Nature* **458**, 1191–1195 (2009).
42. H. M. Kim *et al.*, Crystal structure of the TLR4-MD-2 complex with bound endotoxin antagonist Eritoran. *Cell* **130**, 906–917 (2007).
43. U. Ohto, K. Fukase, K. Miyake, T. Shimizu, Structural basis of species-specific endotoxin sensing by innate immune receptor TLR4/MD-2. *Proc. Natl. Acad. Sci. U.S.A.* **109**, 7421–7426 (2012).
44. A. Penesyan, S. S. Nagy, S. Kjelleberg, M. R. Gillings, I. T. Paulsen, Rapid microevolution of biofilm cells in response to antibiotics. *NPJ Biofilms Microbiomes* **5**, 34 (2019).
45. Y. Sun, D. Shang, Inhibitory effects of antimicrobial peptides on lipopolysaccharide-induced inflammation. *Mediators Inflamm.* **2015**, 167572 (2015).
46. M. R. Scheenstra, R. M. van Harten, E. J. A. Veldhuizen, H. P. Haagsman, M. Coorens, Cathelicidins modulate TLR-activation and inflammation. *Front. Immunol.* **11**, 1137 (2020).
47. M. Marin *et al.*, Human cathelicidin improves colonic epithelial defenses against *Salmonella typhimurium* by modulating bacterial invasion, TLR4 and pro-inflammatory cytokines. *Cell Tissue Res.* **376**, 433–442 (2019).
48. S. Vasoo, J. N. Barreto, P. K. Tosh, Emerging issues in gram-negative bacterial resistance: An update for the practicing clinician. *Mayo Clin. Proc.* **90**, 395–403 (2015).
49. S. M. Opal *et al.*, ACCESS Study Group, Effect of eritoran, an antagonist of MD2-TLR4, on mortality in patients with severe sepsis: The ACCESS randomized trial. *JAMA* **309**, 1154–1162 (2013).
50. F. A. Facchini *et al.*, Structure-activity relationship in monosaccharide-based toll-like receptor 4 (TLR4) antagonists. *J. Med. Chem.* **61**, 2895–2909 (2018).
51. S. Park *et al.*, TLR4/MD2 specific peptides stalled in vivo LPS-induced immune exacerbation. *Biomaterials* **126**, 49–60 (2017).
52. P. F. Slivka *et al.*, A peptide antagonist of the TLR4-MD2 interaction. *ChemBioChem* **10**, 645–649 (2009).
53. T. Kawamoto, M. Ii, T. Kitazaki, Y. Iizawa, H. Kimura, TAK-242 selectively suppresses Toll-like receptor 4-signaling mediated by the intracellular domain. *Eur. J. Pharmacol.* **584**, 40–48 (2008).
54. M. Ali Mohammadie Kojour, Y. S. Han, Y. H. Jo, An overview of insect innate immunity. *Entomol. Res.* **50**, 282–291 (2020).
55. T. Kaneko *et al.*, Monomeric and polymeric gram-negative peptidoglycan but not purified LPS stimulate the Drosophila IMD pathway. *Immunity* **20**, 637–649 (2004).
56. J. Kim *et al.*, Phloretin as a potent natural TLR2/1 inhibitor suppresses TLR2-induced inflammation. *Nutrients* **10**, 868 (2018).